An integrated approach for risk profiling and spatial prediction of *Schistosoma mansoni*–hookworm coinfection

Giovanna Raso*†, Penelope Vounatsou*, Burton H. Singer‡§, Eliézer K. N'Goran¶‖, Marcel Tanner*, and Jürg Utzinger*§

*Department of Public Health and Epidemiology, Swiss Tropical Institute, P.O. Box, CH-4002 Basel, Switzerland; †Molecular Parasitology Laboratory, Queensland Institute of Medical Research, Brisbane, Queensland 4006, Australia; ‡Office of Population Research, Princeton University, Princeton, NJ 08544; ¶Centre Suisse de Recherches Scientifiques, 01 BP 1303, Abidjan 01, Côte d'Ivoire; and ‖UFR Biosciences, Université d'Abidjan–Cocody, 22 BP 770, Abidjan 22, Côte d'Ivoire

Contributed by Burton H. Singer, March 6, 2006

Multiple-species parasitic infections are pervasive in the developing world, yet resources for their control are scarce. We present an integrated approach for risk profiling and spatial prediction of coinfection with *Schistosoma mansoni* and hookworm for western Côte d'Ivoire. Our approach combines demographic, environmental, and socioeconomic data; incorporates them into a geographic information system; and employs spatial statistics. Demographic and socioeconomic data were obtained from education registries and from a questionnaire administered to schoolchildren. Environmental data were derived from remotely sensed satellite images and digitized ground maps. Parasitologic data, obtained from fecal examination by using two different diagnostic approaches, served as the outcome measure. Bayesian variogram models were used to assess risk factors and spatial variation of *S. mansoni*–hookworm coinfection in relation to demographic, environmental, and socioeconomic variables. Coinfections were found in 680 of 3,578 schoolchildren (19.0%) with complete data records. The prevalence of monoinfections with either hookworm or *S. mansoni* was 24.3% and 24.1%, respectively. Multinomial Bayesian spatial models showed that age, sex, socioeconomic status, and elevation were good predictors for the spatial distribution of *S. mansoni*–hookworm coinfection. We conclude that our integrated approach, employing a diversity of data sources, geographic information system and remote sensing technologies, and Bayesian spatial statistics, is a powerful tool for risk profiling and spatial prediction of *S. mansoni*–hookworm coinfection. More generally, this approach facilitates risk mapping and prediction of other parasite combinations and multiparasitism, and hence can guide integrated disease control programs in resource-constrained settings.

multinomial Bayesian geostatistical models | risk mapping and prediction | geographic information system | remote sensing | Côte d'Ivoire

Millions of people in the developing world live at risk of parasitic diseases such as malaria, lymphatic filariasis, soil-transmitted helminthiasis, leishmaniasis, schistosomiasis, trypanosomiasis, Chagas disease, and onchocerciasis (1–3). These diseases are of huge public health and economic significance, and their successful control is an important factor affecting progress toward the United Nations' Millennium Development Goals (3–5). Different combinations of these diseases, as well as other parasitic diseases caused by protozoa, nematodes, trematodes, and cestodes not listed here, and bacterial and viral infectious diseases, often coexist in the same ecoepidemiologic setting (3–7). The causes are multifactorial and include conditions of poverty, poor hygiene status, lack of clean water and adequate sanitation, and difficulty accessing preventive measures and efficacious drugs (8–11). The spatiotemporal distributions of different parasitic infections often overlap, hence polyparasitism is pervasive (4, 6, 12–17).

Although polyparasitism is the norm in tropical and subtropical environments, surprisingly few studies have investigated underlying risk factors that govern the frequency and transmission dynamics of this phenomenon. With the pressing need for systemic approaches to health systems (18), it is necessary to first identify the scope of health problems within communities. Currently, even the best data systems develop only univariate summary tabulations of what in many instances is pervasive comorbidity. Integrated approaches to disease control require an in-depth understanding of spatially explicit risk profiles for simultaneous infection with multiple species of parasites. Efficient management of health systems in resource-constrained areas also requires an effective methodology for predicting the spatial patterns of polyparasitism. For example, a combined approach to treatment of schistosomiasis, soil-transmitted helminthiasis, lymphatic filariasis, and trachoma has been proposed, primarily through large-scale deployment of four safe, efficacious, and inexpensive drugs: praziquantel, albendazole/mebendazole, ivermectin, and azithromycine (3, 4). However, cost-effective distribution of these drugs, and other control measures, require *a priori* knowledge of high-risk areas, where polyparasitism is most prevalent (5).

A basic question linked directly to cost-effective deployment of drugs that has received minimal attention to date is how to rapidly identify communities at elevated risk of multiple-species parasitic infections. The advent of geographic information systems and remote sensing technologies and the progression in geostatistical modeling have opened new avenues for disease risk mapping and spatial prediction, which in turn can guide control interventions (19–24). However, virtually all extant studies and epidemiologic reports focus on the prediction of a single disease. We clearly require validated models that can be used to predict the risk of multiple-species parasitic infections, and hence aid in spatial targeting of control measures.

This article presents an integrated approach to risk profiling, mapping, and prediction of high-risk areas for *Schistosoma mansoni*–hookworm coinfection. We focus on western Côte d'Ivoire, where malaria, schistosomiasis, soil-transmitted helminthiasis (mainly hookworm disease), giardiasis, and amebiasis are common parasitic diseases, and coinfection is the norm (6, 14, 25). The emphasis is on schoolchildren, and we use a diversity of data sources to identify demographic, environmental, and socioeconomic risk factors and integrate them in Bayesian geostatistical models. Our work serves as a prototype for spatially explicit risk mapping and for the prediction of coinfection with multiple species of parasites in general.

Results

Compliance and Final Study Cohort. Of 5,448 children listed on the education registries for grades 3–5 in 57 rural schools of western

Conflict of interest statement: No conflicts declared.

Abbreviations: BCI, Bayesian credible interval; OR, odds ratio; RRR, risk ratio ratio; CI, confidence interval; SAF, sodium–acetic acid–formalin.

§To whom correspondence may be addressed. E-mail: singer@princeton.edu or juerg.utzinger@unibas.ch.

www.pnas.org/cgi/doi/10.1073/pnas.0601559103

Table 1. Observed infection status with *S. mansoni* and/or hookworm, based on a single Kato–Katz thick smear reading, a single SAF-processed stool sample examination, or the two methods combined, among 3,578 schoolchildren in the region of Man, western Côte d'Ivoire

Infection status	Single Kato–Katz thick smear	Single SAF-processed stool sample	Pooled results*
No infection			
No. (%) of children	1,519 (42.5)	2,184 (61.0)	1,167 (32.6)
School range, %	2.0–78.9	20.4–91.4	2.0–70.4
S. mansoni monoinfection			
No. (%) of children	952 (26.6)	461 (12.9)	862 (24.1)
School range, %	0.0–72.2	0.0–45.5	0.0–63.9
Hookworm monoinfection			
No. (%) of children	667 (18.6)	754 (21.1)	869 (24.3)
School range, %	0.0–58.3	0.0–70.2	0.0–65.7
S. mansoni–hookworm coinfection			
No. (%) of children	440 (12.3)	179 (5.0)	680 (19.0)
School range, %	0.0–52.7	0.0–31.5	0.0–60.0

*Both diagnostic approaches combined.

Côte d'Ivoire in the school year 2001/2002, a total of 4,755 (87.3%) were present during the epidemiologic survey and provided a stool sample to the research team. Results from both the Kato–Katz thick smear readings and the sodium–acetic acid–formalin (SAF)-fixed stool samples processed by an ether-concentration method were obtained for 4,336 schoolchildren (79.6%). Complete questionnaire results were obtained from 4,376 schoolchildren (80.3%). The final cohort had 3,578 schoolchildren (65.7%) from 56 schools, and subsequent analyses were performed on this cohort. There were significantly more boys than girls (2,162 vs. 1,416, respectively; $P < 0.001$) in the cohort. With regard to age, 1,956 (54.7%) of the children were aged 6–10 yr and 1,622 (45.3%) were aged 11–16 yr.

Schoolchildren's Infection Status. Table 1 illustrates that pooling the results of the two diagnostic approaches increased the prevalence rates for both *S. mansoni* and hookworm considerably. A total of 1,167 (32.6%) children were free of *S. mansoni* and hookworm infections, 869 (24.3%) had a monoinfection with hookworm, 862 (24.1%) were infected with *S. mansoni* only, and 680 (19.0%) had a coinfection with both parasites. At the unit of the school, the prevalence of coinfection ranged from 0% to 60%. For details on mono- and coinfection prevalence at the 56 schools, please refer to Table 4, which is published as supporting information on the PNAS web site.

Table 2 shows the observed infection status of schoolchildren according to the pooled parasitologic data, stratified by sex and age. The prevalence of mono- and coinfections was significantly higher among boys than girls (likelihood ratio test = 20.07, $P < 0.001$), and older schoolchildren were more likely to harbor either one or both parasite species concurrently than their younger counterparts (likelihood ratio test = 109.11, $P < 0.001$).

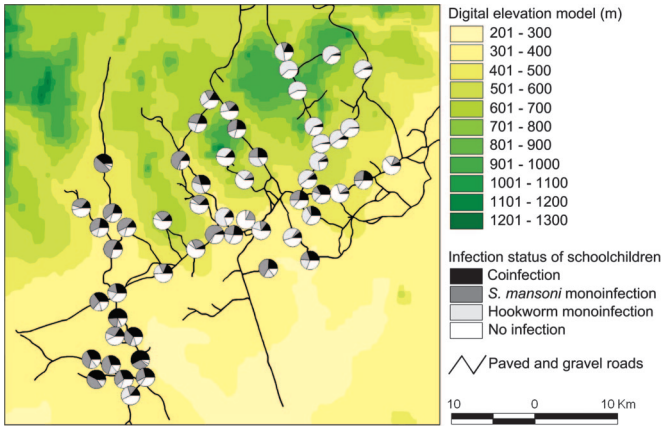

Fig. 1. Distribution of mono- and coinfections with *S. mansoni* and hookworm among 3,578 schoolchildren of 56 rural schools in the region of Man, Côte d'Ivoire.

Fig. 1 depicts the spatial distribution of children's infection status, with the school as the unit of analysis. The highest frequencies of coinfection with *S. mansoni* and hookworm, exceeding 35%, were observed in the southwestern part of the study area.

Multinomial Nonspatial Analyses. Bivariate model results from the multinomial nonspatial analyses showed that sex, age group, socioeconomic status, land cover, elevation, slope, rainfall, land surface temperature, normalized difference vegetation index, soil type, and distance to the nearest health-care facility were significant covariates for a monoinfection with either *S. mansoni* or hookworm, or a coinfection ($P < 0.001$). Distance to permanent rivers also showed a significant association with infection status ($P = 0.013$).

Bayesian Multinomial Spatial Analysis. The significant covariates identified by the multinomial nonspatial models were built into the final Bayesian multinomial spatial model. Table 3 summarizes the resulting significant covariates for either a monoinfection with *S. mansoni* or hookworm, or a coinfection [mean coefficient estimates within Bayesian credible interval (BCI)]. Boys were more likely to have an *S. mansoni*–hookworm coinfection than girls [risk ratio ratio (RRR) = 2.45; 95% BCI, 1.97–3.06], and children aged 11–16 yr had higher odds for a coinfection than their younger counterparts (RRR = 1.55; 95% BCI, 1.25–1.92). Children belonging to the two poorest wealth quintiles were at an ≈2-fold higher risk of a coinfection with *S. mansoni* and hookworm than their less-poor counterparts. With regard to environmental covariates, elevation showed the strongest leverage on an *S. mansoni*–hookworm coinfection; children attending schools at altitudes <400 m were at a 4.5-fold higher risk than those living at higher altitudes. This result is primarily due to the increased risk of

Table 2. Observed infection status with *S. mansoni* and/or hookworm, based on pooled results from the two diagnostic approaches, among 3,578 schoolchildren in the region of Man, western Côte d'Ivoire, stratified by sex and age

	Sex			Age		
Infection status	Male, %	Female, %	*P* value*	6–10 yr, %	11–16 yr, %	*P* value*
No infection	27.5	40.5	<0.001	35.6	29.0	<0.001
S. mansoni monoinfection	22.6	26.3		23.0	25.4	
Hookworm monoinfection	27.2	19.8		23.9	24.7	
S. mansoni–hookworm coinfection	22.7	13.4		17.4	20.9	

**P* values based on likelihood ratio test.

Table 3. Comparison of results between multivariate binomial spatial models for *S. mansoni* and hookworm infections (regardless of infection status with other parasites) and the multivariate multinomial spatial model with categories for monoinfections with *S. mansoni* and hookworm and coinfection with both parasites

		Binomial spatial model				Multinomial spatial model					
		S. mansoni infection (26)		Hookworm infection (27)		*S. mansoni* monoinfection		Hookworm monoinfection		*S. mansoni*–hookworm coinfection	
Data source	Covariate	OR	95% CI	OR	95% CI	RRR	95% BCI	RRR	95% BCI	RRR	95% BCI
School registry	Demography										
	Age										
	6–10 yr	1.00		1.00		1.00		1.00		1.00	
	11–16 yr	1.46*	1.24, 1.71	1.13	0.97, 1.31	1.59†	1.30, 1.96	1.18	0.98, 1.44	1.55	1.25, 1.92
	Sex										
	Female	1.00		1.00		1.00		1.00		1.00	
	Male	1.21	1.03, 1.41	2.06	1.77, 2.39	1.18	0.97, 1.43	2.02	1.66, 2.46	2.45	1.97, 3.06
Questionnaire	Socioeconomic status										
	Most poor	1.00		1.00		1.00		1.00		1.00	
	Very poor	1.12	0.85, 1.44	1.26	0.99, 1.58	0.86	0.61, 1.21	1.08	0.79, 1.49	1.33	0.94, 1.88
	Poor	1.08	0.82, 1.39	0.92	0.72, 1.16	0.84	0.61, 1.17	0.83	0.60, 1.15	0.89	0.63, 1.25
	Less poor	0.91	0.69, 1.18	0.72	0.56, 0.91	0.82	0.59, 1.14	0.74	0.54, 1.04	0.59	0.41, 0.84
	Least poor	0.73	0.55, 0.95	0.66	0.51, 0.85	0.58	0.41, 0.82	0.67	0.48, 0.94	0.41	0.29, 0.60
Ground maps	Elevation										
	<400 m	1.00		1.00		1.00		1.00		1.00	
	≥400 m	0.20	0.07, 0.50	1.66	1.04, 2.52	0.19	0.07, 0.57	2.08	1.30, 3.40	0.22	0.09, 0.54
Satellite images	Land cover type										
	Woody savannah			1.00		1.00		1.00		1.00	
	Tropical forest			1.64	1.06, 2.48	1.08	0.50, 2.36	1.68	1.03, 2.81	1.19	0.58, 2.51
	Deforested savannah and crops			1.51	0.81, 2.62	0.59	0.22, 1.56	1.47	0.78, 2.80	0.77	0.31, 2.00
	Tropical rainforest			1.01	0.49, 2.51	0.86	0.29, 2.61	1.15	0.54, 2.44	0.67	0.24, 1.84
Model variable	σ^{2}‡	1.72		0.43		1.68		0.48		1.31	
	u§	0.40		2.51		0.73		2.34		0.91	

Results are presented as ORs and 95% CIs for the binomial model and as RRRs and 95% BCIs for the multinomial model.

*$OR_{S.\ mansoni} = (p_{ij}/1 - p_{ij})_{(11–16\ yr)}/(p_{ij}/1 - p_{ij})_{(6–10\ yr)} = 1.46$.

†$RRR_{S.\ mansoni} = (p_{ij2}/p_{ij4})_{(11–16\ yr)}/(p_{ij2}/p_{ij4})_{(6–10\ yr)} = 1.59$.

‡σ^2 is the estimate of geographical variability.

§u is a scalar parameter representing the rate of decline of correlation with distance between points.

S. mansoni infections at elevations <400 m, whereas the risk of hookworm infections *per se* is higher at elevations >400 m.

Although tropical forest showed a significant association with hookworm monoinfection, none of the land cover types investigated were significantly associated with either an *S. mansoni* monoinfection or an *S. mansoni*–hookworm coinfection. For comparison, our previous analyses employing a binomial model with an emphasis on *S. mansoni* infections (regardless of hookworm infection status) (26) and hookworm infections (regardless of *S. mansoni* infection status) (27) are also presented in Table 3. With regard to hookworm infections, children belonging to the less-poor wealth quintile had an odds ratio (OR) of 0.72 [95% confidence interval (CI), 0.56–0.91], which was significant in the single-infection model, whereas the RRR of the hookworm monoinfection category of the multinomial model showed no statistical significance (RRR = 0.74; 95% BCI, 0.54–1.04). Furthermore, the OR in the hookworm single-infection model was 1.66 for elevation (27), whereas for monoinfections the RRR was considerably higher, i.e., 2.08. The rate of decline of the spatial correlation for *S. mansoni* was higher in the monoinfection category of the multinomial model compared with the single-infection model (26), whereas the rate of decline of the spatial correlation for hookworm was higher in the single-infection model (27). The distance at which spatial correlation is <5% was 4.1 km for *S. mansoni* monoinfections, 1.3 km for hookworm monoinfections, and 3.3 km for coinfections with both parasites. For comparison, the *S. mansoni* and hookworm infection models in our previous analyses revealed spatial correlations of <5% at distances of 7.5 km (26) and 1.2 km (27), respectively.

Model Validation. By using 95% BCI of the predicted infection prevalence as the designated threshold for model validation, the frequency of children with *S. mansoni*–hookworm coinfection was predicted correctly in all 16 villages (100%). The frequencies of children with either an *S. mansoni* or a hookworm monoinfection were predicted correctly in 15 of 16 villages (93.8%). Finally, the frequencies of no infection were predicted correctly in 14 of 16 villages (87.5%).

Prediction of *S. mansoni*–Hookworm Coinfections. Fig. 2 displays the prevalence of *S. mansoni*–hookworm coinfections resulting from the predictive model with the covariates age group, sex, socioeconomic status, elevation, and land cover types. The prevalence is predicted with an emphasis on high-risk groups, i.e., boys aged 11–16 yr from the poorest households. The largest geographic area, with *S. mansoni*–hookworm coinfection prevalence exceeding 35%, was predicted for the southwestern part of the study area, covering an area of ≈50 km^2. Our model also predicted high prevalence for *S. mansoni*–hookworm coinfections for an area of ≈4 km^2 located southeast of the town of Man. These predicted high-risk areas are in agreement with the parasitologic findings, as shown in Fig. 1.

Fig. 3 displays the standard deviation of the predicted coinfection prevalence. As expected, the error of the prediction was higher with increasing distance from sampled locations.

Discussion

Recent epidemiologic studies confirmed that polyparasitism remains a predominant problem in the developing world (6, 14, 15, 17, 28, 29). These observations provide leverage for inte-

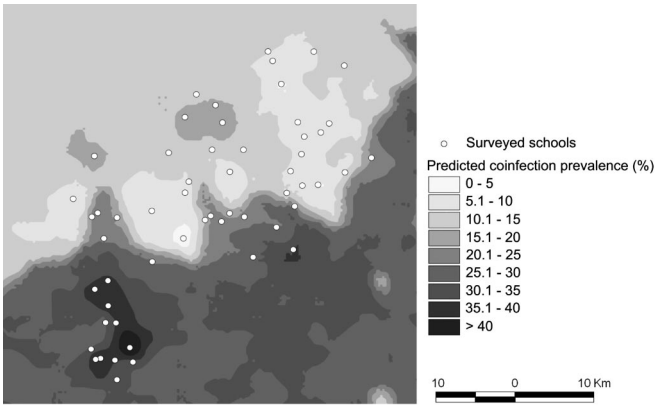

Fig. 2. Map of *S. mansoni*–hookworm coinfection prevalence among schoolchildren in the region of Man, Côte d'Ivoire.

grated control programs, which in turn are likely to contribute to progress toward internationally set targets, such as the Millennium Development Goals (3–5, 30, 31). Yet, little research has been carried out to elucidate the underlying risk factors for multiple-species parasitic infections and their spatial distribution. In an attempt to bridge this gap, we have developed an integrated approach to mapping and predicting the distribution of *S. mansoni*–hookworm coinfection in the region of Man, western Côte d'Ivoire.

Our approach combines demographic, socioeconomic, and environmental data obtained from a diversity of sources, i.e., simple questionnaires, existing education registries, ground maps, and remotely sensed satellite data, and employs spatial statistics by using Bayesian geostatistical models. The prior lack of such an integrated approach might be explained on two grounds. First, the development of geographic information system and remote sensing technologies, and their application to health issues in general and tropical infectious diseases in particular, has a history of only ≈10–15 yr (32–35). Second, significant advances have been made with Bayesian approaches, which allow flexible modeling and inference and provide computational advantages over frequentist analyses via the implementation of Markov chain Monte Carlo methods (36). Bayesian approaches allow spatial dependence to be modeled in a hierarchical fashion, by introducing area- or site-specific random effects with conditional autoregressive (37, 38) or Gaussian random field prior specifications (39). These advances have greatly improved spatial data analysis, including disease risk mapping and prediction at nonsampled locations. For example, Bayesian approaches have been applied successfully to genetic epidemiology and nutritional ecology to explain child growth in Papua New Guinea (40), to malaria risk at different spatial scales in sub-Saharan Africa (41–43), and to map and predict community prevalence of onchocerciasis in the Venezuelan Amazon (44), schistosome prevalence among schoolchildren in Côte d'Ivoire and Tanzania (24, 26), prevalence and intensity of infection with *Schistosoma japonicum* in China and the Philippines (45, 46), and hookworm infections in schoolchildren living in western Côte d'Ivoire (27). Although the previous work applied univariate outcomes (e.g., prevalence data), the present work describes spatially explicit analysis of risk profiling for multinomial outcomes that include coinfection.

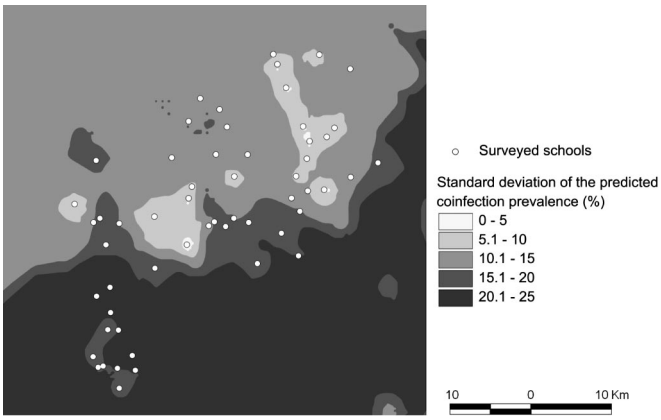

Fig. 3. Map with standard deviation of the predicted *S. mansoni*–hookworm coinfection prevalence among schoolchildren in the region of Man, Côte d'Ivoire.

An overall *S. mansoni*–hookworm coinfection prevalence of 19.0% was found after pooling the results of two different diagnostic techniques: the Kato–Katz technique and the processing of SAF-conserved stool samples by an ether-concentration method. Microscopic examination of Kato–Katz thick smears is the most widely used approach in epidemiologic surveys focusing on intestinal schistosomiasis and soil-transmitted helminthiasis (47). However, this technique is known to lack sensitivity because of significant day-to-day and intraspecimen variation in fecal egg counts of *S. mansoni*, as well as the rapid dissolving of hookworm eggs on microscope slides that are covered with glycerine-soaked cellophane paper (47–51). Indeed, examination of Kato–Katz thick smears singly revealed an *S. mansoni*–hookworm coinfection prevalence of only 12.3% and hence underestimated the "true" coinfection prevalence by 6.7%, or more than one-third. The calculated sensitivity of a single Kato–Katz thick smear and a single SAF reading for the diagnosis of coinfections was 65.9% and 40.1%, respectively (taking the pooled Kato–Katz and SAF results as the "composite reference standard"), when a specificity of 100% is assumed. Although sensitivity is increased when different diagnostic tools are combined or a more extensive sampling effort is undertaken (e.g., multiple Kato–Katz thick smears obtained from consecutive fecal specimens), the infection prevalence in this setting is still likely to be underestimated.

The results of the multinomial geostatistical models suggest that children's socioeconomic status is a significant predictor not only for the spatial heterogeneity of a monoinfection with either *S. mansoni* or hookworm, but also for coinfection with both parasites. The relationship between wealth quintiles and children's infection status is consistent with previous findings from the same study area that also employed Bayesian geostatistical models for mapping and prediction of *S. mansoni* (regardless of other infections) (26) and hookworm (regardless of other infections) (27). We had speculated that children living in less-poor households were more likely to have a latrine at home, and that wealth might influence household decision-making processes [e.g., better access to health care because transportation and treatment fees can be covered more readily (26)]. The present investigation adds further weight to our previous claims, because children belonging to the least-poor wealth quintile were at a significantly lower risk of a coinfection with *S. mansoni* and hookworm than children with no or monoinfections, suggesting that the poorest of the poor may encounter the greatest difficulties in access to health care, clean water, and adequate sanitation. These are important risk factors that govern the spatial distribution of coinfections and must be addressed if further progress toward the Millennium Development Goals is to be made in an equitable manner.

Geographic information systems and remote sensing are increasingly applied to predict the distribution of tropical parasitic diseases, because these techniques facilitate the identification and visualization of environmental indicators for infection risk (22, 23, 52). In the present application, elevation was identified as an important environmental predictor for *S. mansoni*–hookworm coinfection; children attending schools located at elevations <400 m were at a 4.5-fold higher risk of a coinfection than children from higher-

altitude schools. A similar observation had been made in the same study area for *S. mansoni* infection regardless of concurrent hookworm infection status (26). Depending on the topography, elevation can serve as a proxy for the flow velocity of rivers (52), which, in turn, governs the abundance of intermediate host snail habitat. At low elevations, flow velocity may drop below a critical threshold, e.g., 0.3 m/sec, at which snail populations can survive (53). Conversely, because elevation may act as proxy for increased rainfall in the mountainous area, higher flow velocities usually occur with increasing altitude (26, 27).

Although multiparasitism is the norm in the developing world, only limited attempts have been made to shed light on the interrelationships between multiple-species infections and morbidity and comorbidity (15). Further research is warranted on the burden caused by coinfections, to derive better estimates of the cost-effectiveness of interventions. We have developed an integrated approach and used Bayesian geostatistical multinomial models for risk profiling and for mapping and prediction of the spatial distribution of *S. mansoni*–hookworm coinfection. The resulting risk maps can identify villages where access to efficacious drugs, combined with the provision of clean water and adequate sanitation, is most needed, and where introduction of such measures can yield the greatest payoff by targeting schistosomiasis and hookworm disease simultaneously. More generally, our integrated approach can be adapted to other parasite combinations and, if successfully validated in other ecoepidemiologic and socioeconomic settings, can establish itself as a cornerstone for integrated parasitic disease control programs.

Materials and Methods

Study Area and Population. The study was carried out from May to August 2002 in the region of Man, a mountainous area located in western Côte d'Ivoire. Recent cross-sectional surveys conducted in this setting confirmed that infections with *S. mansoni* and hookworm are common (6, 14, 54, 55). Study participants were 6- to 16-yr-old children attending grades 3–5 at 57 rural schools.

Ethical Approval and Consent. The study protocol was approved by the institutional review boards of the Swiss Tropical Institute (Basel) and the Centre Suisse de Recherches Scientifiques (Abidjan, Côte d'Ivoire). Ethical clearance was granted by the Ministry of Health in Côte d'Ivoire. After the study aims and procedures were explained, written informed consent was obtained from the two education officers. The officers then informed school directors about the study, and detailed information was provided by our research team on the day preceding the parasitologic survey.

Data Sources: Demography, Environment, and Socioeconomic Status. Schoolchildren's demographic data (i.e., age and sex) were readily available from education registries, which were made available by the education officers.

Schoolchildren's socioeconomic status was obtained by teachers administering a questionnaire that included a list of assets owned (e.g., possession of a radio) and household characteristics (e.g., walls constructed with bricks). An asset-based approach, in accordance with a previously described method, allowed stratification of schoolchildren into wealth quintiles (56).

The geographic coordinates of each school were collected by using a handheld global positioning system (Thales Navigation, Santa Clara, CA). Streets, village boundaries, rivers, elevation lines, and soil types were digitized from existing ground maps at scales of 1:50,000 to 1:500,000. Land cover types were obtained from the Advanced Very High Resolution Radiometer (AVHRR) satellite; U.S. Geological Survey (USGS) Africa Land Cover Characteristics Database v.2: Africa Seasonal Land Cover Regions; and USGS Earth Resources Observation System (EROS) Data Center at 1 × 1-km spatial resolution. Normalized difference vegetation index and land surface temperature data were downloaded at 1 × 1-km spatial resolution from the Moderate Resolution Imaging Spectroradiometer (MODIS) from the USGS EROS Data Center. Rainfall estimate data with an 8 × 8-km spatial resolution, from the Meteosat 7 satellite, were obtained from the Africa Data Dissemination Service. Normalized difference vegetation index, land surface temperature, and rainfall estimate data were downloaded for the period September 2001 to August 2002 and processed as detailed (26, 27).

Outcome Measure: Children's Infection Status. A cross-sectional epidemiologic survey was carried out to assess children's infection status with *S. mansoni* and hookworm. A single stool specimen was collected from each schoolchild and processed by the following two-pronged diagnostic approach. First, a single 42-mg Kato–Katz thick smear was prepared from each stool sample on microscope slides (57). Slides were allowed to clear for 30–45 min before examination under a light microscope at low magnification. Eggs of *S. mansoni* and hookworm were counted separately and recorded. Other soil-transmitted helminths (i.e., *Ascaris lumbricoides* and *Trichuris trichiura*) were also examined quantitatively, but because of their low frequencies they were not considered further. Second, a 1- to 2-g portion of stool was fixed into 10 ml of SAF, processed with a standard ether-concentration method, and analyzed under a light microscope for helminth eggs and intestinal protozoa (58, 59). Only the presence or absence of *S. mansoni* and hookworm was considered here.

Anthelmintic Treatment. Parasite-positive children received treatment; praziquantel at a single oral dose of 40 mg/kg was given against infection with *S. mansoni*, and a single tablet of albendazole (400 mg) was given to children who had a soil-transmitted helminth infection (60). Drug administration followed a treatment schedule developed recently by the regional health authorities, as described (55).

Data Management and Statistical Analysis. Data obtained from the epidemiologic and questionnaire surveys were double-entered and cross-checked with EPIINFO V.6.04 (Centers for Disease Control and Prevention, Atlanta). Schoolchildren were classified into two age categories, with group 1 consisting of children aged 6–10 yr and group 2 consisting of children aged 11–16 yr. A child was recorded as positive for an infection with *S. mansoni* or hookworm if at least one egg was detected in the Kato–Katz thick smear or the SAF-processed stool sample. The pooled parasitologic data (combined Kato–Katz thick smear and SAF readings) were considered the "composite reference standard" and used in all subsequent analyses. An outcome variable was created with the following four categories: (*i*) coinfection with *S. mansoni* and hookworm, (*ii*) monoinfection with *S. mansoni*, (*iii*) monoinfection with hookworm, and (*iv*) no infection. Environmental covariates were standardized with a mean of 0 and an SD of 1.

For each available demographic, socioeconomic, and environmental covariate, a multinomial model was fitted on the outcome variable in STATA V.8.0 (Stata, College Station, TX). Independent location random effects for each multinomial category with an exchangeable correlation structure were added to model extra-multinomial variation due to geographic correlation. All covariates significant at 0.2 significance level were built into a Bayesian spatial multinomial regression model for a monoinfection with either *S. mansoni* or hookworm and for a coinfection with both parasites, by using WINBUGS V.1.4 (Imperial College and the Medical Research Council, London). Spatial heterogeneity was introduced on the variance–covariance matrix of the random effects. Key model parameters have been summarized with their posterior median and 95% BCI (27, 61).

Let Y_{ijk} and p_{ijk} be the infection status and probability of coinfection ($k = 1$), an *S. mansoni* monoinfection ($k = 2$), a hookworm monoinfection ($k = 3$), and no infection ($k = 4$) of

schoolchild j in village i. We assumed that Y_{ijk} arises from a multinomial distribution, i.e.,

$$(Y_{ij1}, Y_{ij2}, Y_{ij3}, Y_{ij4}) \sim \text{Mult}(1, p_{ij1}, p_{ij2}, p_{ij3}, p_{ij4}), \quad [1]$$

and modeled the influence of covariates $\underline{X}_{ijk}$ and village-specific random effects ϕ_{ik} on the $\log(p_{ijl}/p_{ij4})$, $l = 1, 2, 3$, as

$$\log\left(\frac{p_{ijl}}{p_{ij4}}\right) = \underline{X}_{ij}^T\underline{\beta} + \phi_{il},$$

where $\underline{\beta} = \{\underline{\beta}_l\}_{l=1,2,3} = (\underline{\beta}_1, \underline{\beta}_2, \underline{\beta}_3)$ is the vector of regression coefficients corresponding to the multinomial categories, and p_{ijl}/p_{ij4} is the risk ratio of the infection status with regard to no infection. We introduced a spatial correlation structure on $\underline{\phi} = \{\underline{\phi}_l\}_{l=1,2,3}$ by assuming that $\underline{\phi}_l = (\phi_{1l}, \phi_{2l}, \ldots, \phi_{Nl})^T$ has a multivariate normal distribution, $\underline{\phi}_l \sim \text{MVN}(\underline{0}, \Sigma_l)$, with variance–covariance matrix Σ_l. We also assumed an isotropic spatial process, i.e.,

$$(\Sigma_l)_{ir} = \sigma_l^2 \exp(-u_l d_{ir}),$$

where d_{ir} is the Euclidean distance between villages i and r, σ_l^2 is the geographic variability known as the sill, and u_l is a smoothing parameter that controls the rate of correlation decay with increasing distance. The range of geographic dependency, i.e., the minimum distance at which spatial correlation between locations is $<5\%$ for each category l, was calculated as $3/u_l$ (in meters).

In accordance with a Bayesian model specification, we adopted prior distributions for the model parameters. We choose vague normal prior distributions for the $\underline{\beta}$ parameters with large variances (i.e., 10,000), inverse gamma priors for $\{\sigma_l^2\}_{l=1,2,3}$, and uniform priors for $\{u_l\}_{l=1,2,3}$. Markov chain Monte Carlo simulation was used to estimate the model parameters (36). We ran a single chain sampler with a burn-in of 5,000 iterations. Convergence was assessed by inspection of ergodic averages of selected model parameters. Covariates from the multivariate model were used to generate smooth risk maps of either mono- or coinfections by using Bayesian kriging (39).

Model Validation. Validation was carried out by using a training sample derived from the current database, i.e., 40 locations (71.4%) to establish a spatial model and the remaining 16 locations (28.6%) for prediction. The accuracy of the prediction was determined by comparing observed and predicted prevalence in the 16 test locations. The infection prevalence for a particular test location was defined as correctly predicted if the observed prevalence of this location was within the 95% BCI resulting from the predictive posterior distribution of that location.

We thank the education officers, the directors and teachers of the schools surveyed, and the field and laboratory team (A. Allangba, A. Fondio, K. L. Lohourignon, F. Sangaré, B. Sosthène, and M. Traoré). This work was supported by the Claire Sturzenegger–Jean Favre Foundation, the Novartis Foundation, the Roche Research Foundation through a fellowship to G.R., and Swiss National Science Foundation support to G.R. (Project PBBSB-109011), P.V. (Project 3252B0-102136), and J.U. (Project PP00B-102883).

1. Remme, J. H. F., Blas, E., Chitsulo, L., Desjeux, P. M. P., Engers, H. D., Kanyok, T. P., Kengeya Kayondo, J. F., Kioy, D. W., Kumaraswami, V., Lazdins, J. K., *et al.* (2002) *Trends Parasitol.* **18,** 421–426.
2. World Health Organization (2004) *The World Health Report 2004: Changing History* (W.H.O., Geneva).
3. Hotez, P. J., Molyneux, D. H., Fenwick, A., Ottesen, E., Ehrlich Sachs, S. & Sachs, J. D. (2006) *PLoS Med.* **3,** e102.
4. Molyneux, D. H., Hotez, P. J. & Fenwick, A. (2005) *PLoS Med.* **2,** e336.
5. Utzinger, J. & de Savigny, D. (2006) *PLoS Med.* **3,** e112.
6. Raso, G., Luginbühl, A., Adjoua, C. A., Tian-Bi, N. T., Silué, K. D., Matthys, B., Vounatsou, P., Wang, Y., Dumas, M. E., Holmes, E., *et al.* (2004) *Int. J. Epidemiol.* **33,** 1092–1102.
7. Gallagher, M., Malhotra, I., Mungai, P. L., Wamachi, A. N., Kioko, J. M., Ouma, J. H., Muchiri, E. & King, C. L. (2005) *AIDS* **19,** 1849–1855.
8. Esrey, S. A., Potash, J. B., Roberts, L. & Shiff, C. (1991) *Bull. W.H.O.* **69,** 609–621.
9. Utzinger, J., Bergquist, R., Xiao, S. H., Singer, B. H. & Tanner, M. (2003) *Lancet* **362,** 1932–1934.
10. Thapar, N. & Sanderson, I. R. (2004) *Lancet* **363,** 641–653.
11. Rudan, I., Lawn, J., Cousens, S., Rowe, A. K., Boschi-Pinto, C., Tomaškovic, L., Mendoza, W., Lanata, C. F., Roca-Feltrer, A., Carneiro, I., *et al.* (2005) *Lancet* **365,** 2031–2040.
12. Buck, A. A., Anderson, R. I. & MacRae, A. A. (1978) *Tropenmed. Parasitol.* **29,** 61–70.
13. Keusch, G. T. & Migasena, P. (1982) *Rev. Infect. Dis.* **4,** 880–882.
14. Keiser, J., N'Goran, E. K., Traoré, M., Lohourignon, K. L., Singer, B. H., Lengeler, C., Tanner, M. & Utzinger, J. (2002) *J. Parasitol.* **88,** 461–466.
15. Ezeamama, A. E., Friedman, J. F., Olveda, R. M., Acosta, L. P., Kurtis, J. D., Mor, V. & McGarvey, S. T. (2005) *J. Infect. Dis.* **192,** 2160–2170.
16. McKenzie, F. E. (2005) *Int. J. Epidemiol.* **34,** 221–222.
17. Fleming, F. M., Brooker, S., Geiger, S. M., Caldas, I. R., Correa-Oliveira, R., Hotez, P. J. & Bethony, J. M. (2006) *Trop. Med. Int. Health* **11,** 56–64.
18. Task Force on Health Systems Research (2004) *Lancet* **364,** 997–1003.
19. Carter, R., Mendis, K. N. & Roberts, D. (2000) *Bull. W.H.O.* **78,** 1401–1411.
20. Brooker, S., Hay, S. I. & Bundy, D. A. P. (2002) *Trends Parasitol.* **18,** 70–74.
21. Gemperli, A., Vounatsou, P., Kleinschmidt, I., Bagayoko, M., Lengeler, C. & Smith, T. (2004) *Am. J. Epidemiol.* **159,** 64–72.
22. Malone, J. B. (2005) *Parassitologia (Rome)* **47,** 27–50.
23. Castro, M. C., Monte-Mór, R. L., Sawyer, D. O. & Singer, B. H. (2006) *Proc. Natl. Acad. Sci. USA* **103,** 2452–2457.
24. Clements, A. C. A., Lwambo, N. J. S., Blair, L., Nyandindi, U., Kaatano, G., Kinung'hi, S., Webster, J. P., Fenwick, A. & Brooker, S. (2006) *Trop. Med. Int. Health* **11,** 490–503.
25. Utzinger, J., N'Goran, E. K., Marti, H. P., Tanner, M. & Lengeler, C. (1999) *Trans. R. Soc. Trop. Med. Hyg.* **93,** 137–141.
26. Raso, G., Matthys, B., N'Goran, E. K., Tanner, M., Vounatsou, P. & Utzinger, J. (2005) *Parasitology* **131,** 97–108.
27. Raso, G., Vounatsou, P., Gosoniu, L., Tanner, M., N'Goran, E. K. & Utzinger, J. (2006) *Int. J. Parasitol.* **36,** 201–210.
28. Waikagul, J., Krudsood, S., Radomyos, P., Radomyos, B., Chalemrut, K., Jonsuksuntigul, P., Kojima, S., Looareesuwan, S. & Thaineau, W. (2002) *Southeast Asian J. Trop. Med. Public Health* **33,** 218–223.
29. Tchuem Tchuenté, L. A., Behnke, J. M., Gilbert, F. S., Southgate, V. R. & Vercruysse, J. (2003) *Trop. Med. Int. Health* **8,** 975–986.
30. Molyneux, D. H. & Nantulya, V. M. (2004) *Br. Med. J.* **328,** 1129–1132.
31. Ehrenberg, J. P. & Ault, S. K. (2005) *BMC Public Health* **5,** 119.
32. Malone, J. B., Huh, O. K., Fehler, D. P., Wilson, P. A., Wilensky, D. E., Holmes, R. A. & Elmagdoub, A. I. (1994) *Am. J. Trop. Med. Hyg.* **50,** 714–722.
33. Hay, S. I., Omumbo, J. A., Craig, M. H. & Snow, R. W. (2000) *Adv. Parasitol.* **47,** 173–215.
34. Rogers, D. J. & Randolph, S. E. (2003) *Nat. Rev. Microbiol.* **1,** 231–237.
35. Paolino, L., Sebillo, M. & Cringoli, G. (2005) *Parassitologia (Rome)* **47,** 171–175.
36. Gelfand, A. E. & Smith, A. F. M. (1990) *J. Am. Stat. Assoc.* **85,** 398–410.
37. Bernardinelli, L. & Montomoli, C. (1992) *Stat. Med.* **11,** 983–1007.
38. Gelfand, A. E. & Vounatsou, P. (2003) *Biostatistics* **4,** 11–25.
39. Diggle, P. J., Tawn, J. A. & Moyeed, R. A. (1998) *J. R. Stat. Soc. C* **47,** 299–326.
40. Vounatsou, P., Smith, T. & Gelfand, A. E. (2000) *Biostatistics* **1,** 177–189.
41. Diggle, P., Moyeed, R., Rowlingson, B. & Thomson, M. (2002) *J. R. Stat. Soc. C* **51,** 493–506.
42. Kleinschmidt, I., Sharp, B., Mueller, I. & Vounatsou, P. (2002) *Am. J. Epidemiol.* **155,** 257–264.
43. Nobre, A. A., Schmidt, A. M. & Lopes, H. F. (2005) *Environmetrics* **16,** 291–304.
44. Carabin, H., Escalona, M., Marshall, C., Vivas-Martinez, S., Botto, C., Joseph, L. & Basanez, M. G. (2003) *Bull. W.H.O.* **81,** 482–490.
45. Carabin, H., Marshall, C. M., Joseph, L., Riley, S., Olveda, R. & McGarvey, S. T. (2005) *Am. J. Trop. Med. Hyg.* **72,** 745–753.
46. Yang, G. J., Vounatsou, P., Zhou, X. N., Tanner, M. & Utzinger, J. (2005) *Int. J. Parasitol.* **35,** 155–162.
47. Booth, M., Vounatsou, P., N'Goran, E. K., Tanner, M. & Utzinger, J. (2003) *Parasitology* **127,** 525–531.
48. Martin, L. K. & Beaver, P. C. (1968) *Am. J. Trop. Med. Hyg.* **17,** 382–391.
49. Engels, D., Sinzinkayo, E. & Gryseels, B. (1996) *Am. J. Trop. Med. Hyg.* **54,** 319–324.
50. Utzinger, J., Booth, M., N'Goran, E. K., Müller, I., Tanner, M. & Lengeler, C. (2001) *Parasitology* **122,** 537–544.
51. Raso, G., N'Goran, E. K., Toty, A., Luginbühl, A., Adjoua, C. A., Tian-Bi, N. T., Bogoch, I. I., Vounatsou, P., Tanner, M. & Utzinger, J. (2004) *Trans. R. Soc. Trop. Med. Hyg.* **98,** 18–27.
52. Brooker, S. & Michael, E. (2000) *Adv. Parasitol.* **47,** 245–288.
53. Appleton, C. C. (1978) *Malacol. Rev.* **11,** 1–25.
54. Utzinger, J., N'Goran, E. K., Ossey, Y. A., Booth, M., Traoré, M., Lohourignon, K. L., Allangba, A., Ahiba, L. A., Tanner, M. & Lengeler, C. (2000) *Bull. W.H.O.* **78,** 389–398.
55. Raso, G., Utzinger, J., Silué, K. D., Ouattara, M., Yapi, A., Toty, A., Matthys, B., Vounatsou, P., Tanner, M. & N'Goran, E. K. (2005) *Trop. Med. Int. Health* **10,** 42–57.
56. Filmer, D. & Pritchett, L. H. (2001) *Demography* **38,** 115–132.
57. Katz, N., Chaves, A. & Pellegrino, J. (1972) *Rev. Inst. Med. Trop. São Paulo* **14,** 397–400.
58. Allen, A. V. H. & Ridley, D. S. (1970) *J. Clin. Pathol.* **23,** 545–546.
59. Marti, H. P. & Escher, E. (1990) *Schweiz. Med. Wochenschr.* **120,** 1473–1476.
60. World Health Organization (2002) *W.H.O. Tech. Rep. Ser.* **912,** 1–57.
61. Basáñez, M. G., Marshall, C., Carabin, H., Gyorkos, T. & Joseph, L. (2004) *Trends Parasitol.* **20,** 85–91.